The Role of Oxygen Transport in Atherosclerosis and Vascular Disease

John Tarbell[1], Marwa Mahmoud[1], Andrea Corti[1], Luis Cardoso[1], Colin Caro[2]

[1] Biomedical Engineering Department, The City College of New York, New York, USA
[2] Department of Bioengineering, Imperial College London, UK

Abstract

Atherosclerosis and vascular disease of larger arteries are often associated with hypoxia within the layers of the vascular wall. In this review, we begin with a brief overview of the molecular changes in vascular cells associated with hypoxia and then emphasize the transport mechanisms that bring oxygen to cells within the vascular wall. We focus on fluid mechanical factors that control oxygen transport from lumenal blood flow to the intima and inner media layers of the artery, and solid mechanical factors that influence oxygen transport to the adventitia and outer media via the wall's microvascular system - the vasa vasorum (VV). Many cardiovascular risk factors are associated with VV compression that reduces VV perfusion and oxygenation. Dysfunctional vasa vasorum neovascularization in response to hypoxia contributes to plaque inflammation and growth. Disturbed blood flow in vascular bifurcations and curvatures leads to reduced oxygen transport from blood to the inner layers of the wall and contributes to the development of atherosclerotic plaques in these regions. Recent studies have shown that hypoxia inducible factor 1 α (HIF1-α), a critical transcription factor associated with hypoxia, is also activated in disturbed flow by a mechanism that is independent of hypoxia. A final section of the review emphasizes hypoxia in vascular stenting that is used to enlarge vessels occluded by plaques. Stenting can compress VV leading to hypoxia and associated intimal hyperplasia. To enhance oxygen transport during stenting, new stent designs with helical centerlines have been developed to increase blood phase oxygen transport rates and reduce intimal hyperplasia. Further study of the mechanisms controlling hypoxia in the artery wall may contribute to the development of therapeutic strategies for vascular diseases.

Introduction and Background

The hypoxia theory of atherosclerosis proposes that an imbalance between the demand for and supply of oxygen in the arterial wall is a key factor in the development of intimal hyperplasia and atherosclerotic plaques. Recent review papers [1, 2] have described the biomolecular mechanisms that advance atherosclerotic plaques in the presence of hypoxia. There is substantial evidence that there are regions within the atherosclerotic plaque in which significant hypoxia exists that may change the function, metabolism, and responses of many of the cell types found within the developing plaque, and dictate whether the plaque will evolve into a stable or unstable phenotype.

Hypoxia-Inducible-Factor 1 α (HIF-1α) is a transcription factor that orchestrates the hypoxic response in cells and has been regarded as the 'Master Regulator of Hypoxia' (Fig. 1). Under normoxic conditions (physiological levels of oxygen), HIF-1α becomes targeted for degradation through proline hydroxylation by HIF prolyl hydroxylase (PHD) which results in a conformational change promoting its binding to Von Hippel–Lindau disease tumour suppressor protein (VHL) E3 ligase complex, which in turn targets HIF-1α for ubiquitination and rapid proteasomal degradation. In hypoxia, HIF-1α degradation is inhibited, resulting in its accumulation in the cells, leading to its nuclear translocation and HIF1-α target gene expression. HIF-1α target genes mediate inflammation, proliferation, angiogenesis and glycoclysis[3].

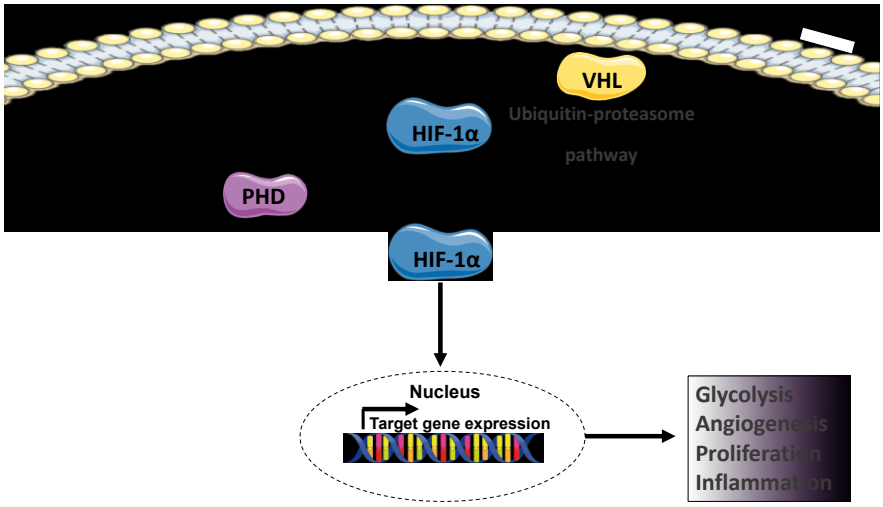

Figure 1. Schematic representation of hypoxic signaling. In normoxia, HIF-1α becomes targeted for degradation through proline hydroxylation by HIF prolyl hydroxylase (PHD). This results in a conformational change in HIF-1α, promoting its binding to Von Hippel–Lindau disease tumour suppressor protein (VHL) E3 ligase complex, and targeting HIF-1α for ubiquitination and rapid proteasomal degradation. In hypoxia, HIF-1α degradation is inhibited, resulting in its accumulation in the cells, and leading to its nuclear translocation and HIF1-α target gene expression. HIF-1α target genes mediate changes in cell function leading including proliferation,

Inflammatory disease states are often characterized as either being a result of tissue hypoxia or in activating hypoxia [4]. Thus, it is not surprising that hypoxia and inflammation share common signaling pathways; of major importance is NF-κB activation. It was first reported in 1994 by Koong et al that hypoxia activates NF-κB signaling by triggering the degradation of inhibitory IκB-a, resulting in the release of p65 (RelA) from the inhibitory complex and translocation into the nucleus where it promotes the transcription of NF-κB target genes [5]. Since then, there have been numerous studies that demonstrate the activation of the inflammatory NF-κB pathway in hypoxia (reviewed in [4] [6]). Consistent with this, it has also been shown that NF-κB signaling triggers HIF-1α activation in immune cells. In response to macrophage stimulation by bacterial infection, lipopolysaccharides (LPS) or hypoxia, active NF-κB signalling triggers the activation of HIF-1α [7, 8]. In endothelial cells, non-canonical hypoxic signaling triggered by disturbed blood flow in the vasculature results in the activation of HIF1-a through NF-κB [9]. Interestingly, both NF-κB and HIF-1α can be activated by the same stimuli, this includes proinflammatory cytokines such as TNF-α and Interleukin-6, oxidative stress and disturbed blood flow [8, 9].

In concert with inflammation, hypoxia also triggers glucose metabolic changes in cells. Under low oxygen levels this change in metabolism is required to maintain adequate ATP production in cells [10]. Under inflammatory conditions, HIF-1α triggers the activation of glycolysis genes in endothelial cells [9]. In macrophages the production of LPS by bacterial infection triggers glycolysis through HIF1-α [7].

In endothelial cells, the glycolysis shift caused by HIF-1α gives rise to enhanced cell proliferation and inflammation [9, 11]. HIF1-α also triggers endothelial-mesenchymal transition [12] [13], a process that results in further enhancement of inflammation, proliferation and permeability and has been shown to trigger atherosclerosis [14] [15]. All of these changes in endothelial cell function are a hallmark of a dysfunctional endothelium which leads to the development of atheroscelrosis.

While the biomolecular mechanisms relating hypoxia to atherosclerosis have been well described, the biophysical mechanisms responsible for hypoxia and its localization to regions of the vasculature where atherosclerosis develops have received less attention. Thus a major aim of this review is elucidate the biophysical mechanisms responsible for hypoxia, and to suggest methods to ameliorate hypoxia that derive from biophysical understanding.

We begin with a discussion of the pathways for oxygen transport to the arterial wall emphasizing transport to the inner layers from luminal blood flow and the outer layers from the supporting microvascular network – the vasa vasorum. The role of vasa

vasorum compression leading to medial layer hypoxia in vascular disease is elucidated and the pathways for inflammatory response and plaque development provided by the vasa vasorum are described. Impaired blood phase oxygen transport characteristics in regions of branching and curvature where atherosclerotic plaques localize are then discussed. It is well known that these are regions of disturbed flow that induce endothelial cell dysfunction, and recent studies show that even HIF1α is upregulated by disturbed flow. But here it is emphasized that these are typically regions of vessel wall hypoxia as well. The final sections of the review deal with vascular stenting that reduces downstream hypoxia but can induce vessel wall hypoxia, intimal hyperplasia and re-stenosis within the stented region. The effects of stent expansion on vasa vasorum compression and reduced blood flow to the outer layers of the wall are reviewed. A final section describes the biophysical effects of a stent with a helical centreline that promotes enhanced oxygen transport to the inner layers of the wall by virtue of the secondary flows induced by the helical geometry and reduces intimal hyperplasia.

Pathways for Oxygen Transport to the Arterial Wall

There are two principal pathways for oxygen transport to the arterial wall: the inner layers (intima and inner media) receive oxygen primarily from lumenal blood flow and the outer layers (adventitia and outer media) from vasa vasorum, a microvascular network whose principal function is to service the outer regions of thicker blood vessels (Fig. 2 left).

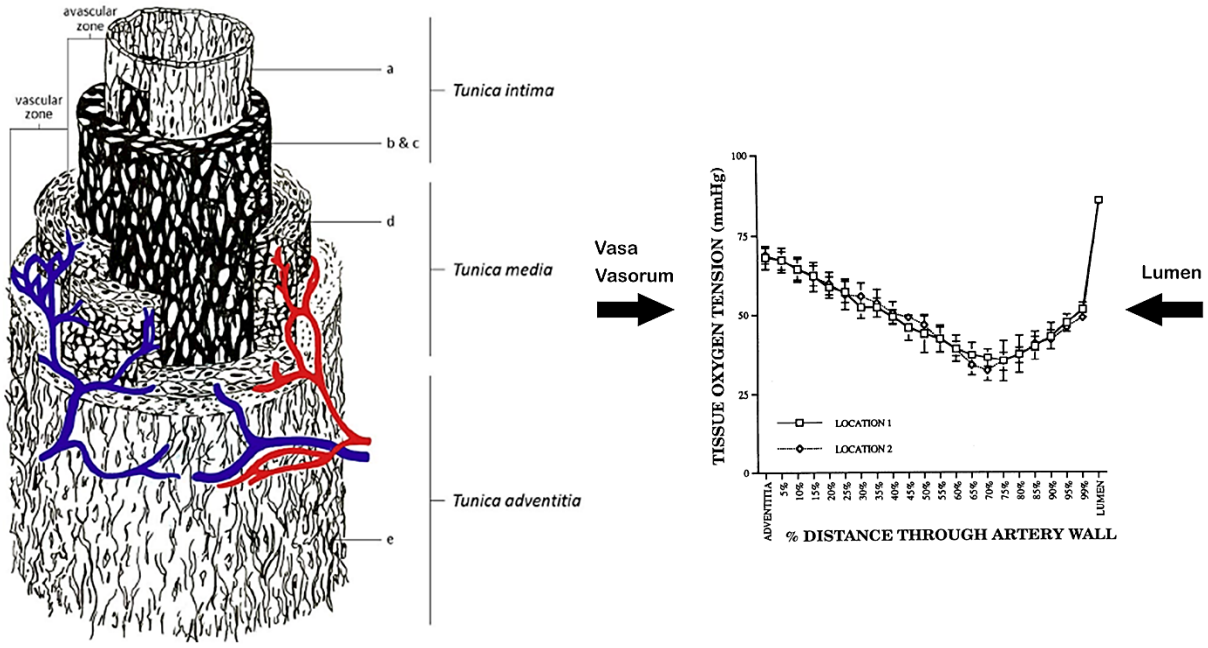

Figure 2. Two main pathways for oxygen transport to the blood vessel wall. (Left) The intima and inner media are supplied from the luminal blood whereas the adventitia and outer media are supplied by the vasa vasorum. [16] (Right) Arterial wall oxygen tension profile in the common carotid artery of a dog. [17]

Depending on their origin, VV are divided into three categories [18] : Vasa Vasorum Interna VVI, when the origin is the main lumen itself and the branching network remains inside the arterial wall; Vasa Vasorum Externa VVE, when the origin is located outside the vascular wall and comes from a major branch emerging from the main lumen; Venous Vasa Vasorum VVV, when the tree structure starts from a neighboring vein. The pattern of vasa vasorum penetration into the outer layers of the wall is dependent on the wall thickness. Wolinsky and Glagov (1967) examined thoracic aortic segments of 12 mammalian species and observed that mammals whose aortas had 29 or fewer medial lamellar units had no demonstrable intramural vascular channels (penetrating vasa vasorum); those whose aortas had more than 29 medial lamellar units, had medial vasa vasorum [19]. Aortas with medial vasa vasorum always had a subintimal medial zone devoid of vasa vasorum. Remarkably, the thickness of the avascular zone was about 0.47 mm in all species, suggesting that diffusive transport from the inner most vasa vasorum and the lumen is limited to this distance. Williams and Heistad (1988) pointed out that in normal arteries, vasa vasorum from the adventitia grow into the media of large arteries and veins and actively regulate blood flow to the wall of these vessels [20]. But in atherosclerotic arteries, vasa vasorum proliferate into the intima-media, where they provide nutrition to the thickened artery. These neovascular channels are thin-walled, however, and may contribute to intraplaque hemorrhage, plaque disruption, and mural thrombosis. Choi et al. identified macrophages and microchannels in mild coronary atherosclerosis supporting the role of inflammation and vasa vasorum proliferation in the early stage of coronary atherosclerosis [21].

Niinikoski et al. demonstrated that a transarterial wall oxygen gradient is present in normal rabbit aortas with oxygen tensions falling from the adventitia, reaching a nadir at the junction of the inner one-third and outer two-thirds of the vessel wall [22]. This was demonstrated more clearly with oxygen microelectrode measurements by Santilli et al. (1995)[17]. A typical oxygen tension profile across a healthy artery (in this case the common carotid artery of a dog) is displayed in Figure 2 (right). Oxygen tension drops precipitously from the lumen to the inner most regions of the wall suggesting a significant oxygen transport resistance in the wall region of the lumen. This is followed by a more gradual drop in oxygen tension in the inner layers as oxygen supplied from the lumen is consumed by the cells in the media (primarily smooth muscle cells in the un-diseased artery). The oxygen tension also drops gradually in the outer layers as fibroblasts and smooth muscle cells consume oxygen. The steadily falling oxygen tensions away from the adventitial surface suggest that the carotid artery wall is not supplied by any penetrating vessels from the vasa vasorum. This is expected because the reported thickness of the vessel segment (0.204 mm) is well below the expected avascular zone thickness (0.47 mm) reported by Wolinsky and Glagov (1967) [19]. This was supported by light-microscopic examination which revealed vasa vasorum only on the adventitial surface.

The role of oxygen transport pathways in vascular disease

Transport from the Vasa Vasorum

Early studies in the aortic media of dogs (Heistad et al.,1978 [23] indicated that vasa vasorum provide a considerable amount of blood flow to the outer wall layers of' the

thoracic aorta. The vessels were responsive to physiologic stimuli as they dilated during infusion of adenosine and constricted during acute hypertension. They speculated that reduction of blood flow to the aortic wall via the vasa vasorum in hypertension might contribute to aortic medial necrosis.

Booth et al. (1989) [24] developed a model of atherosclerosis by positioning a hollow silastic collar around the carotid artery of cholesterol-fed rabbits resulting in macrophage and smooth muscle cell infiltration into the arterial subendothelium, foam cell formation and deposition of extracellular lipid, all in the presence of a morphologically intact endothelium. They proposed that the changes induced by the collar were mediated by obstruction of the adventitial vasa vasorum and the creation of localized wall hypoxia. This concept of vasa vasorum occlusion leading to outer wall ischemia and progression to atherosclerosis was further elaborated by Martin et al. (1991) [25].

Analytical and numerical modeling of the deformation of venous and arterial vasa vasorum were developed by Maurice et al. (1998) [26]. A nonlinear elastic vessel wall model showed that a normal range of intraluminal pressure induces a small deformation in the vasa vasorum in arteries but a larger deformation in venous vasa vasorum. Increased luminal pressure was predicted to compress vasa vasorum and reduce flow thereby resulting in reduced oxygen transport to the outer wall. More recently, Ritman and Lerman (2007) [18] stressed that acute modulation of vasa vasorum patency due to surrounding compressive forces within vessel wall and due to variable tone in the smooth muscle affect the progression of atherosclerotic plaques.

Compressive stress (tone) in the arterial media that may induce vasa vasorum deformation and wall hypoxia has been assessed indirectly through pulse wave velocity (PWV) measurements relying on the classical Moens-Korteweg formula that relates PWV to the elastic modulus (Young's modulus E) of the wall as described in (eqn. 1), where h is the wall thickness, r is artery radius and ρ is the density.

$$PWV = \sqrt{\frac{E \cdot h}{2r\rho}} \tag{1}$$

Caro et al. (1987) [27], by means of non-invasive multichannel doppler ultrasound measurements of PWV, showed that cigarette smoking in healthy subjects increases arterial wall stiffness (E). In a related study Tarnawski et al. (1998) [28]observed increased PWV in subjects with a nicotine patch. Bouthier et al. (1984) found that PWV was increased significantly in hypertensive subjects compared to normotensive controls. Tarnawski et al. (1994) [29] determined significantly higher PWV in non-athletes compared to age-matched athletes. Psychosocial stress/anxiety have also been shown to increase PWV (Logan et al., 2012) [30]. All of these factors that increase PWV are considered risk factors for cardiovascular disease. Szymigielski et al. (2016) [31] showed that pulse wave velocity correlates with aortic atherosclerosis as characterized by intimal-medial thickness. The implication of these studies is that increased vessel

wall compression associated with elevated PWV (E) compresses vasa vasorum leading to outer wall hypoxia and vascular dysfunction.

The Vasa Vasorum in atherosclerotic plaque development

The initiation and progression of atheromas [32-34] is characterized by elevated plasma lipid concentration (hypercholesterolemia)[35] and increased transport of low density lipoprotein (LDL) across an impaired endothelium [36, 37]. Dysfunctional endothelium develops under the influence of hypertension, free radicals, and inappropriate flow shear stress. Contrary to the long standing believe that the vast majority of LDL transport occurs at the luminal side of the vessel, recent studies have shown that adventitial VV play a significant role in the initiation and/or progression of vascular disease [38, 39]. Endothelial dysfunction in both the arterial lumen and the arterial vasa vasorum leads to delivery of LDL, oxidized and inflammatory products, at a rate [40] greater than the clearance by venous vasa vasorum [41]. Phagocytes are attracted into the vessel wall, and a chronic vascular inflammatory environment (i.e. increased expression of NF-κB) initiates the process of local plaque formation [42]. Another consequence of infiltration of lipids, accumulation of macrophages, release of cytokines and angiogenic stimulus generated by oxidative stresses in the vessel wall is the proliferation of vasa vasorum [43-47]. Accumulation of inflammatory cells in the intima stimulates the proliferation of smooth muscle cells in the media, and as a consequence, the vessel wall undergoes positive remodeling, increasing its wall thickness.

Thickening of the vessel wall changes the transmural pressure gradient and wall tissue stresses, and creates regions with low oxygen tension in the medial layer [48, 49], where metabolic needs exceed the amount of oxygen that can diffuse from the lumen [50, 51]. The blood flow resistance is high in the distal vasa vasorum located close to the media layer. High wall tissue stresses within the intima and medial layers of the wall can exceed the blood pressure in the vasa vasorum at that location, and significantly restrict blood flow through them. Also, VV blood flow may be selectively reduced by increased smooth muscle tone in proximal vasa vasorum due to inflammation or thrombosis. These mechanisms can result in insufficient removal of waste products and local hypoxia in the media layer.

Reduced perfusion from the vasa vasorum promotes increased progression of fatty streaks, further increasing oxygen demand [52] in the intima layer, resulting in local hypoxia. Thus, higher VV density is required to meet the oxygen perfusion needs of the arterial wall. Hypoxia triggers local vasa vasorum neovascularization via the production of angiogenic factors. Studies in hypertensive rats demonstrated increase in HIF-1α and angiogenic factors [43, 45-47], including VEGF expression in the aorta, which was subsequently followed by increase in vasa vasorum density around the aorta [53]. A similar increase in HIF-1α and VEGF has been demonstrated in coronary arteries in hypercholesterolemic pigs [54]. Reversibility of endothelial dysfunction at the early stages of atherosclerosis is associated with a reduction in vasa vasorum density (neovascularization). Moreover, anti-angiogenic therapy reduced plaque

neovascularization and plaque growth [55], and it was associated with a reduction of macrophages in the plaque and around the vasa vasorum [20, 56].

Neovascularization within atherosclerotic plaques leads to VV that are immature. These vessels lack a smooth muscle cell layer, tight junctions and a continuous basement membrane [57]. Dysfunctional VV lead to stasis of blood flow, loss of endothelial barrier function, increased vascular permeability and extravasation of fluids and proteins [58, 59]. Unfortunately, proliferation of ruptured and/or leaky vasa vasorum seems to facilitate the ingress of pro-atherogenic cellular and soluble plasma components, including macrophages and inflammatory factors into the vessel wall, thus further enhancing angiogenesis [56] and the progression of atherosclerosis [60]. Leaky VV within the atheroma core lead to intraplaque hemorrhage [57, 61, 62]. Extravasated erythrocytes come in contact with plaque lipid, and undergo hemolysis followed by oxidation of hemoglobin and release of free heme or iron, which accumulates within the plaque [63]. Also, hemoglobin/heme released from phagocytosed erythrocytes by macrophages contributes to the iron deposition in lesions [64], necrotic core size and increased macrophage density [65]. Vasa vasorum hemorrhage is a key factor in the development of unstable atherosclerotic lesions [65, 66]. VV is two-fold denser in vulnerable plaques and four-fold denser in ruptured plaques, when compared to stable plaques [67, 68].

In summary, initiation and progression of VV neovascularization in atherosclerosis is driven by both chronic inflammatory and hypoxic environments within the tissue [69, 70]. Angiogenesis of VV is a physiological response of the organism to restore the appropriate nutrition and oxygen supply in the vessel wall; however, dysfunctional VV neovascularization (i.e. increased intraplaque VV density with impaired endothelium) further contributes to plaque inflammation [71], intraplaque hemorrhage [65], thin-cap fibroatheromas [62] and acute cardiovascular events [57, 62].

Transport from the Lumen

Experiments in dogs (Santilli et al., 1995)[17] show significant induction of inner wall hypoxia in the disturbed flow region of the internal carotid artery (carotid sinus) compared to the common carotid artery, and reduction of inner wall hypoxia in the stable flow region of the internal carotid (Fig. 3). The hypoxic region in the carotid sinus (region 3 in Fig. 3) has been shown to be a region of low fluid wall shear stress compared to the common carotid artery, whereas region 4 is characterized by higher shear stress [72, 73]. These observations suggest that fluid phase transport of oxygen to the blood vessel wall is controlling oxygen tension in the inner wall region. This hypothesis is suggested by the Leveque theory of mass transport in thin boundary layers [74] indicating that the rate of fluid phase oxygen transport to the wall, as characterized by the mass transport coefficient k_L (see Fig. 4), is proportional to the wall shear rate (wall shear stress / viscosity) to the 1/3 power. And, it is well known that region (3) develops atherosclerotic plaques whereas regions (1) and (4) are typically spared [75, 76].

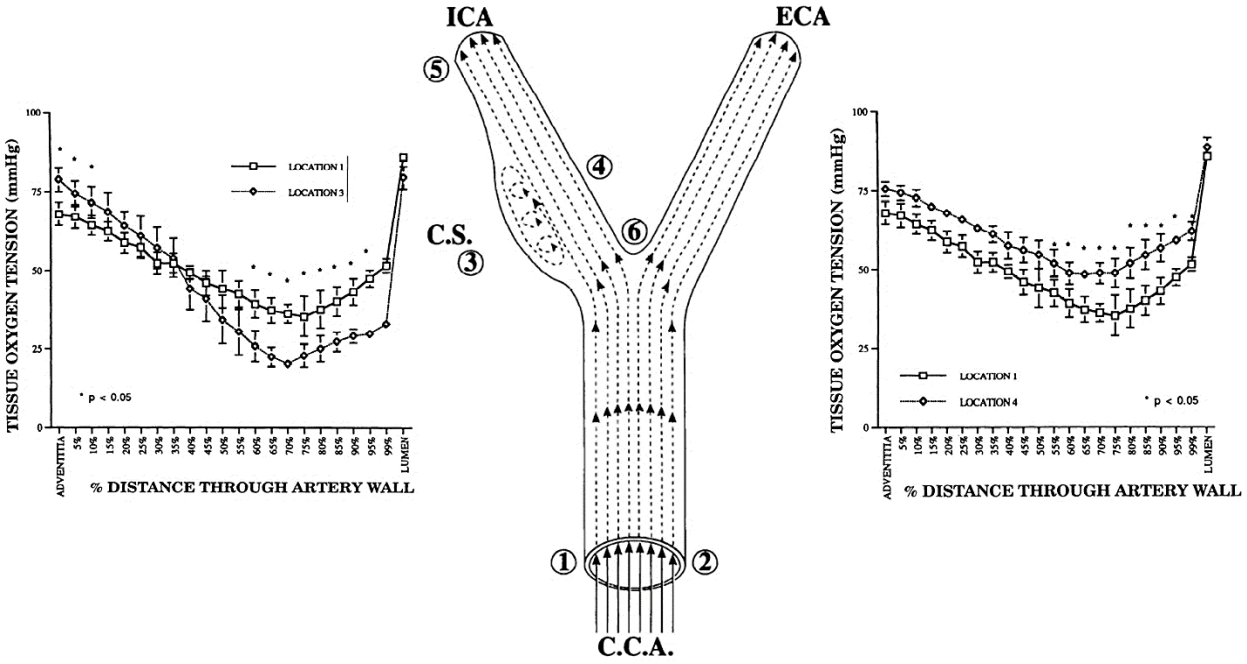

Figure 3. Intra-arterial oxygen tension profiles in dog carotid artery. (Left) Comparison of profiles in the common carotid (position 1) and the disturbed flow carotid sinus (position 3). (Right) Comparison of profiles in the common carotid (position 1) and the stable flow inner wall (position 4). From Santilli et al.[17].

The theory of fluid phase transport to an artery wall has been elaborated in several studies. Tarbell (2003) [77] presented a simplified analysis that is summarized in Figure 3. By assuming that endothelial cells offer no transport resistance for highly diffusible oxygen ($C_w = C_s$) and that oxygen consumption by cells in the wall is the limiting rate process within the wall (oxygen diffusion is rapid), a simple expression for the surface concentration relative to the bulk concentration is obtained

$$\frac{C_s}{C_b} = 1 - \frac{Da_w}{Sh} \tag{2}$$

In eqn (2), the Damhkoler numer (Da_w) is the dimensionless wall oxygen consumption rate and the Sherwood number (Sh) is the dimensionless fluid phase mass transfer coefficient. For a fixed oxygen consumption rate (fixed Da_w), when the fluid phase mass transfer rate is large ($Sh >> Da_w$) then $C_s \rightarrow C_b$ and there is no limitation from fluid phase mass transport (the wall consumption is limiting). However, for lower rates of fluid phase transport, $Sh \rightarrow Da_w$, and $C_s \rightarrow 0$ (the blood phase mass transport is limiting). Note that equation (1) predicts negative surface concentrations when $Sh < Da_w$. This derives from an assumption in the analysis that PO_2 in the tissue is well above the value of the Michaelis constant in a Michaelis – Menten description of the kinetics of oxygen consumption. The Michaelis constant is typically of order 1 mm Hg [78] and PO_2 in the

deep wall is well above that level (see Fig. 2). Values for Da_w based on data in the literature for oxygen consumption in arteries range between 11 and 49 [77].

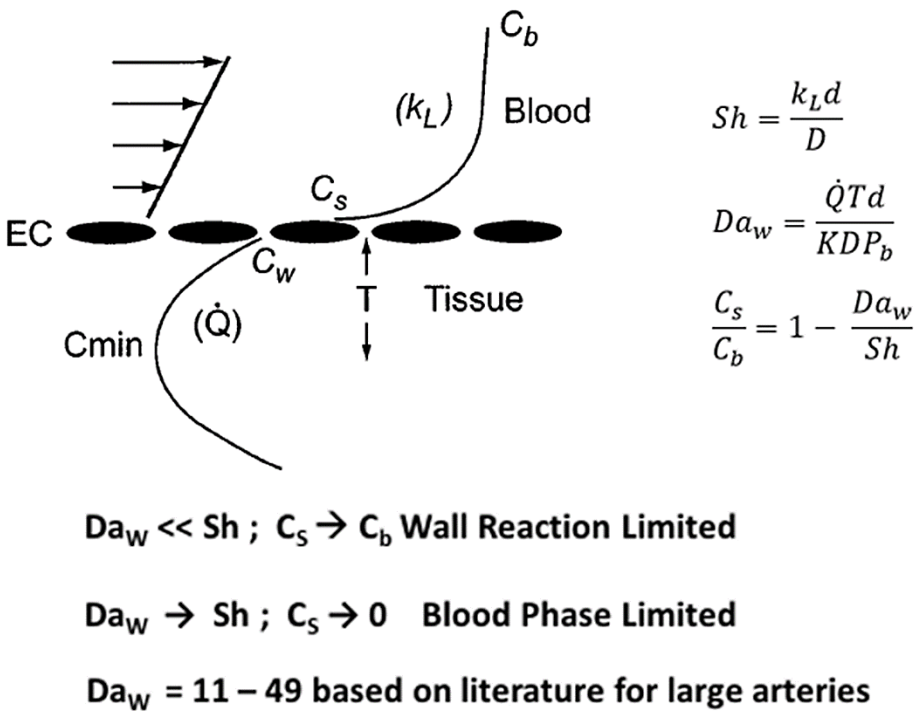

Figure 4. Outline of Simplified Mass Transport Considerations for Oxygen Transport to a Blood Vessel Wall. The schematic displays the concentration profile from the bulk blood (C_b) to the endothelial cell surface (C_s) to the inner wall (C_w) and the minimum value (C_{min}) as indicated in figure 2. k_L is the fluid phase mass transport coefficient, $\dot{Q}$ is the oxygen consumption rate, T is the distance to C_{min} – roughly ½ the wall thickness. The velocity profile at the left is linearized because of the thin concentration boundary layer (Leveque approximation). The Sherwood number or dimensionless mass transfer coefficient introduces the vessel lumen diameter (d) and oxygen diffusion coefficient in the tissue (D). The Damkholer number (Da_w) is the dimensionless *oxygen* consumption rate within the wall and P_b is the bulk oxygen tension (related to C_b through the Henry's law relationship C=KP, where K is the Henry's law constant).

Subsequent detailed computer simulations of oxygen transport in the carotid bifurcation, neglecting oxygen binding to hemoglobin (Tada and Tarbell [79] , revealed more clearly the fluid phase transport limitations in the carotid sinus (Fig 5). The color coded concentration profiles show a uniform PO_2 entry profile at 90 mm Hg. The wall boundary condition was taken to be zero, consistent with an assumption of fluid phase transport limitation. The cross sectional oxygen concentration distributions are shown in the 4 panels at the top of the figure. There is a clear prediction of reduced fluid phase oxygen concentration in the carotid sinus region that is consistent with the observations in

Figure 3. The Sherwood number (Sh) calculations show regions of highly reduced Sh in the carotid sinus along with regions of elevated Sh on the opposite wall – again quite consistent with the data in figure 2. Note also that regions of low Sh co-localize with regions of low wall shear stress (WSS) although there is not a complete overlap of the two regions (Fig. 5 right). Moore and Ethier [80] had pointed out inaccuracies associated with the neglect of hemoglobin binding but they do not alter the basic conclusions of Tada and Tarbell [79].

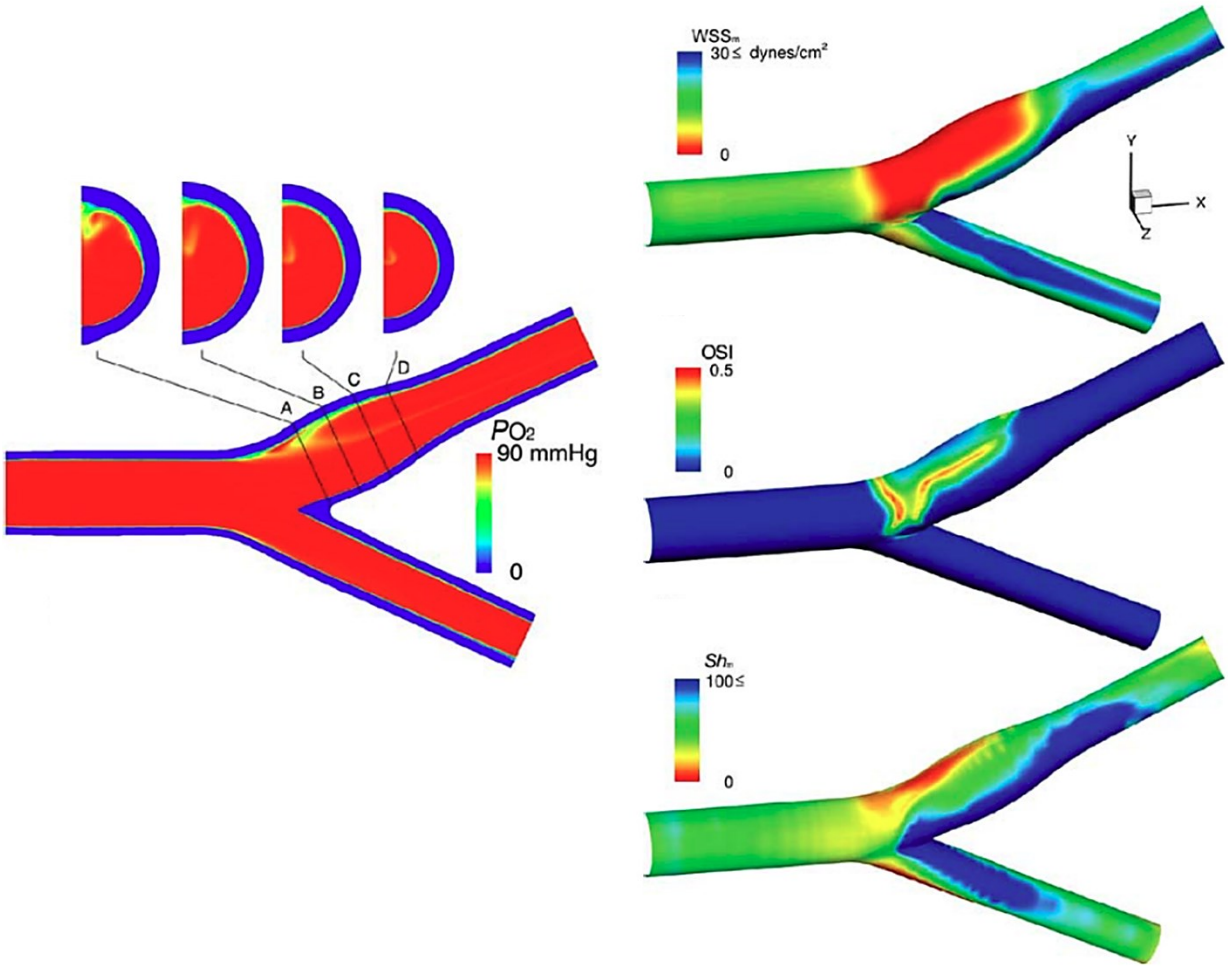

Figure 5. Computer simulations of fluid phase oxygen transport in the carotid bifurcation. Color coding on the left panels indicates PO_2 levels. Note in the right panel that red is indicative of low Sh and blue of high Sh. Based on Tada and Tarbell [79]

Related computer simulations for a curved artery approximating the curvature of a coronary artery over the surface of the heart have been described [81]. For typical coronary artery curvatures, flow conditions and transport properties characteristic of oxygen, the results indicate a large difference in Sherwood number between the outside

(Sh about 55) and inside (Sh about 2) walls, implying that O2 transport at the inner wall could be limited by the fluid phase. More generally, the inner curvature of arteries is also a region of relatively low wall shear stress [9] and a site for localization of atherosclerosis [82].

Disturbed Flow Activates HIF1α

Although HIF-1α activation by hypoxia is the canonical pathway, interestingly a number of recent studies revealed that HIF-1α can be activated non-canonically, through mechanical activation. Wu et al. show that disturbed blood flow (which exerts a low, oscillating shear stress on the surface of endothelial cells lining arteries) in porcine arteries led to elevated levels of HIF-1α [11]. Consistent with this, Feng et al show that HIF-1α was also elevated at sites of disturbed flow in porcine and murine arteries [9]. A study by Fernandez et al., show that HIF-1α was enhanced in endothelial cells exposed to disturbed flow located at the fibrosa side of the aortic valve of human patients [83]. These studies revealed that HIF-1α can be activated by disturbed blood flow *in vivo.* In addition, these studies, using *in vitro* flow systems that recapitulate the shear stress *in vivo,* show that endothelial cells exposed to disturbed flow under normoxic conditions had elevated HIF-1α mRNA and protein levels [9, 11, 83]. Thus, it appears from these findings that both hypoxia induced by disturbed flow, and disturbed flow itself can induce HIF-1α expression.

The activation of HIF-1α by disturbed flow is linked to the induction of endothelial cell dysfunction and subsequent atherogenesis and calcific aortic valve disease. In response to disturbed flow, HIF-1α has been shown to be activated through NFκB proinflammatory signalling, along with stabilization by the debiquitinating enzyme cezanne [9]. Elevated HIF-1α levels in turn trigger the activation of glycolysis genes, leading to a metabolic reprogramming of cells and elevated levels of inflammation and proliferation, and these in turn are hallmarks of a dysfunctional endothelium which promotes atherogenesis [9, 11]. Wu et al suggest that the mechanism by which disturbed flow activates HIF-1α is through reactive oxygen species (ROS) generating oxidase NOX4, which leads to elevated HIF-1α levels and downstream activation of proinflammatory NFκB signaling, enhanced glycolysis and endothelial cell dysfunction [11]. Interestingly HIF-1α activation by disturbed flow can be controlled epigenetically. Fernandez et al show that downregulation of miR483 by disturbed flow leads to elevated HIF-1α levels in endothelial cells through enhanced expression of a miR483-target gene UBE2C, which functions as a ubiquitinating protein that degrades VHL, leading to HIF-1α accumulation. Elevated HIF-1α levels promote inflammation and endothelial-mesenchymal-transition in endothelial cells, leading to dysfunction and calcification in the aortic valve [83].

Non-canonical activation of HIF-1α by disturbed flow appears to play an important role in the progression of disease. However, it also appears that these proatherogenic disturbed flow areas are hypoxic, and that disturbed flow along with hypoxia play a dual

role in switching on HIF-1α-mediated endothelial cell dysfunction leading to disease progression in arteries.

Stent Hypoxia

The most reliable treatment for symptomatic vascular narrowing is percutaneous transluminal angioplasty (PTA), which widens the narrowed sections of the artery using a catheter balloon and often placing a medical stent, a slender, expandable, cylindrical metal mesh in the region of vascular occlusion [84]. The stent works as a mechanical support for the vascular wall, re-opening the pathological region and restoring the original blood flow. However, PTA with stenting is often complicated by in-stent restenosis secondary to neointimal hyperplasia, which may result in failure of the implant. Although restenosis is linked to different aspects of the procedure, recent studies have highlighted the relationship between reduced levels of oxygen tension within the stented artery wall and intimal hyperplasia [85-89]. The stent itself plays a key role in determining the overall oxygen supply to the underlying tissue. Even though the stent restores the required blood flow to downstream vasculature, it may induce a hypoxic condition for the arterial layers around the stent.

It is widely believed that intimal hyperplasia following stenting is the result of an inflammatory response to intimal damage during stent implantation and expansion [90, 91] as well as a material reaction in the case of polymer coated stents [92]. The initial IH response occurs rapidly (within 1 week) and may become significant at 1-3 months. In addition, decreased oxygen tensions have been noted throughout the artery wall immediately following stent deployment with a return toward control values at 28 days in a rabbit model (Fig. 6). Larger stent deployment diameters yielded acutely lower artery wall oxygen tensions.

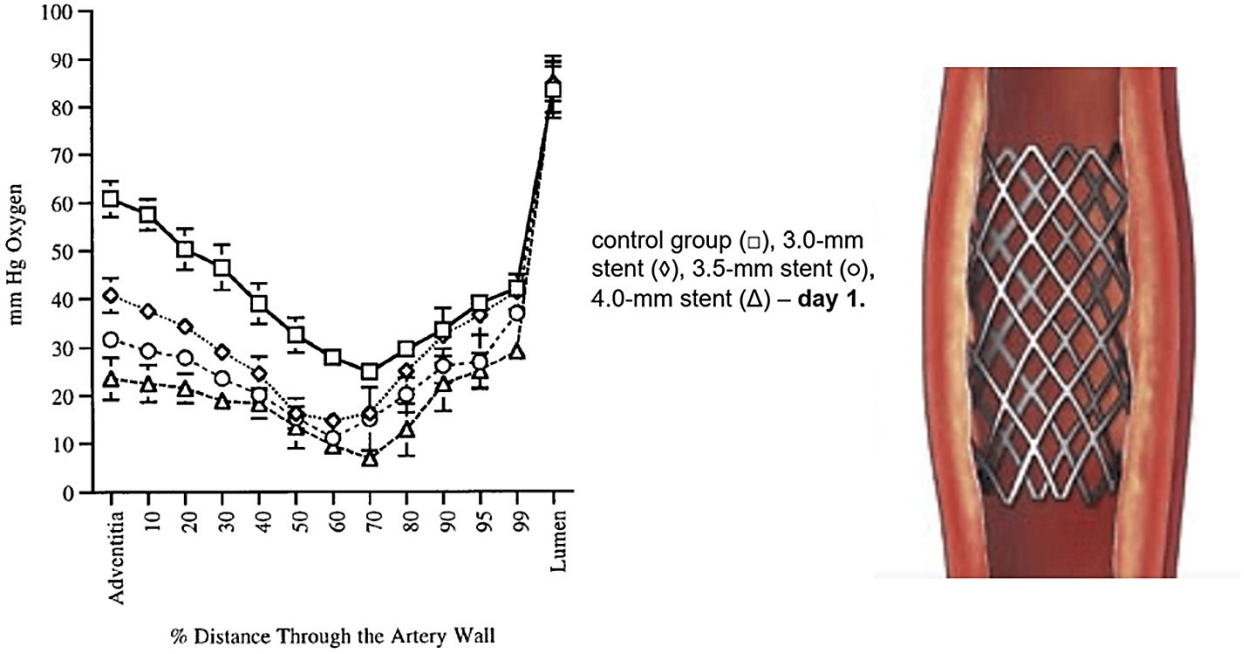

Figure 6. Stent expansion induces outer wall hypoxia. Oxygen tension data at various stent expansions in the distal aorta of rabbits at 1 day after stenting [88].

Inner wall hypoxia during stenting appears to be driven by increased smooth muscle cell oxygen consumption associated with cellular compression during the acute phase of response (days) after stent deployment [88]. This increased demand for oxygen can lead to a supply limitation from the blood phase as discussed in the context of figure 2. In addition, inner wall hypoxia may be associated with reduced fluid phase transport driven by local flow separation around stent struts [86, 93]. The endothelial layer is also damaged during stenting [94], but the endothelium itself offers very little resistance to oxygen transport and is not expected to be influential in controlling wall hypoxia [77].

Outer wall hypoxia appears to be driven by reduced oxygen transport through the vasa vasorum. It has been suggested, but not observed directly, that VV deformation associated with increased wall compression in stenting is responsible for outer wall hypoxia. This mechanism would be exaggerated in stent overexpansion as possibly reflected in Santilli [88] showing greater outer wall hypoxia with stent overexpansion (Fig. 6).

Cheema et al. [87] showed that outer wall hypoxia after stenting leads to up-regulation of VEGF and PDGF inducing an angiogenic response that ultimately increases outer wall microvessel density over a period of 4 weeks. This may in part account for the observed reduction in outer wall hypoxia after 4 weeks of stenting observed by Santilli et al. [88]. However, this mechanism provides a new pathway for inflammatory response, macrophage infiltration and associated wall thickening that may exacerbate intimal hyperplasia as discussed in the earlier section on vasa vasorum in atherosclerotic plaque development.

Consistent with evidence for wall hypoxia after stenting is the recent report of Li et al. [95] who showed that hyperbaric oxygen therapy after coronary stenting improved patient’s myocardial circulation compared to a control group with stents but without oxygen therapy. Earlier work in rabbits had shown that supplemental oxygen reduces IH after stent deployment [89]. Additional work in rabbits indicated that supplemental oxygen inhibits IH and SMC proliferation after creation of an arterio-venous fistula and prolongs patency [96].

Deformation of Vasa Vasorum after Stenting

Previous research has focused its attention on understanding the effect of disruption of blood flow through Vasa Vasorum [97-99]. The results are often medial necrosis, stagnant interstitial fluid, decreased vascular wall nutrition, and wall hypoxia. All of these may occur when the artery is stent-expanded. Stent-expanded arteries may reach sufficiently elevated degrees of deformation such that high circumferential and radial stresses could compress VV thus diminishing blood flow through VV and reducing oxygen delivery to the outer layers of the vessel wall. During stent expansion, circumferential stresses in the layers remain rather small as long as the elastic fibers

are able to stretch. Once they reach the maximum extension, the stress begins to increase exponentially as collagen, which is 100 to 1,000 times stiffer than elastin, bears increasing load [88]. On the other hand, radial stress is the compressive component responsible for squeezing the structures in the artery wall. Increments in both circumferential and radial stresses likely affect the original VV morphology, and may contribute to artery wall hypoxia. This mechanism naturally implies a relation between final stent diameter, arterial stress and VV diameter that could provide the link between transarterial wall oxygen gradient and the degree of stent expansion [88, 99]. In clinical practice, stents are routinely expanded under fluoroscopy to achieve a stent/artery luminal diameter ratio of 1.1:1. However, it can happen that the implant exceeds this limit, reaching a situation of overexpansion where the ratio is 1.2:1 or greater. Stent expansion may compress the Vasa Vasorum, resulting in reduction of vascular wall blood perfusion leading to wall hypoxia. Previous studies have used Finite Element Analysis (FEA) to investigate the mechanical interaction between expanded stents and atherosclerotic tissues[100-102]. Others have focused on the influence of the implant design on the heamodynamics and oxygen transport rates through the stented lumen[86, 99].

A very recent study implemented FEA to explore Vasa Vasorum compression induced by stenting, assessing whether the final stent diameter could induce a hypoxic situation in the outer vascular layers [103]. An idealized multi-layered fibroatheroma model was created (Fig. 7 left) comprising the Intima, Media, and Adventitia layers as thick walled non-linear elastic cylindrical tubes. The plaque was modeled as a semi-annular lipid core placed in the intimal layer, causing a 60% stenosis. Four Vasa Vasorum trees were oriented symmetrically around the vessel (top – opposite the plaque, bottom – under the plaque, left and right) with three branches of decreasing diameter in the axial and radial direction, penetrating into each vascular layer. The stent was expanded to reach a stent/artery lumen diameter ratio of 1.1:1, 1.2:1 and 1.3:1 in different simulations. The results indicated large increases in resistance to blood flow (pressure drop / flow) with stent expansion. Assuming the pressure drop between the VV inlet and outlet remain constant, the blood flow would drop more than 4 times in the Media and Intima when considering the in-series network organization of longitudinal, descending branches (Fig. 7 right). These increases in hydraulic resistance could potentially lead to a hypoxic condition, especially when the stent is over-expanded.

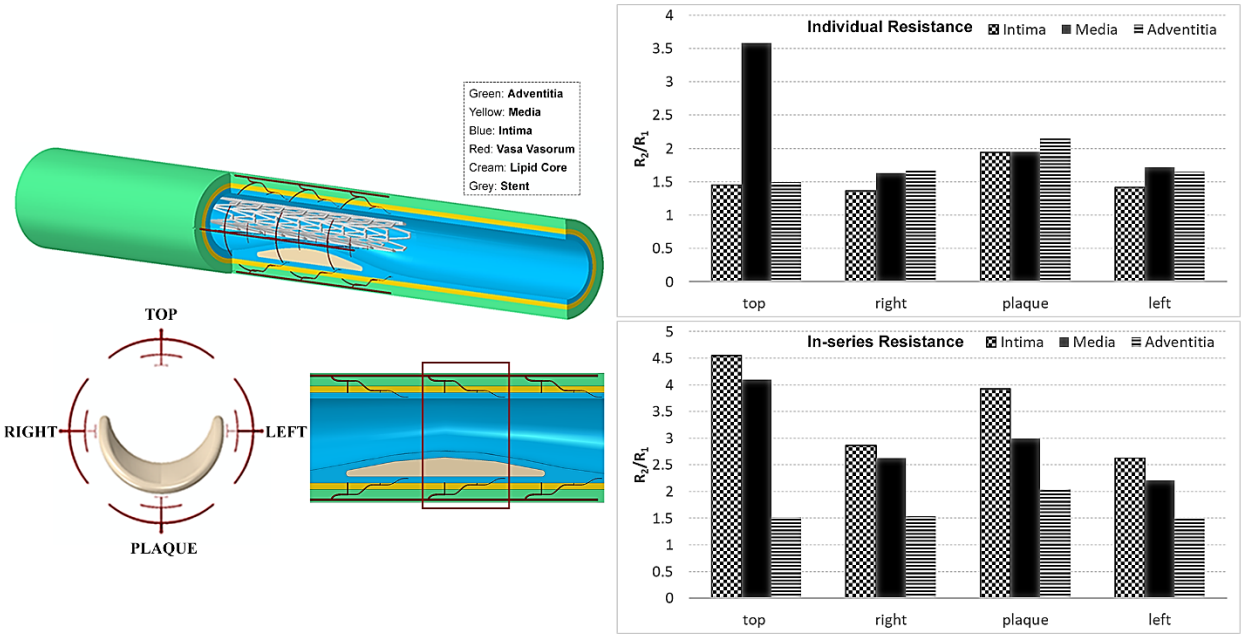

Figure 7. (left) Illustration of the plaque, VV, stent model in lateral section. (right) Fold increase in resistance to flow (pressure drop/flow) for over-expanded stent (1.3:1). Histograms report both the individual change in resistance at each layer (right top) and the resulting augmentation due to the vessels in-series layout (right-bottom). Results refer to VV in the central region in the red rectangle (left) ([103]).

Altered Stent Geometry Enhances Fluid Phase Mass Transport

In addition to anti-proliferative[104] and anti-inflammatory [105] drug release from stents to suppress IH, and hyperbaric oxygen to directly ameliorate the effects of hypoxia on IH after stenting [95], an approach based on alteration of blood flow mechanics and blood phase oxygen transport rates was introduced by Shinke et al. [106] and described in greater detail by Coppola and Caro (2009) [85, 107] and Caro et al. (2013). They modified a commercially available bare-metal, nitinol, self-expanding stent by introducing a helical-centreline geometry (Fig 8 left). The helical geometry induces secondary flows (in the plane perpendicular to the axial flow) that alter fluid shear stress and mass transport characteristics. The new stent design was initially tested in straight sections of pig common carotid arteries with a conventional straight centerline stent in one CCA and the helical stent in the contralateral CCA. After 30 days there was a 45% reduction in intimal thickness associated with the helical stent compared to the straight stent (Fig. 8 right). In addition, there was a 40% reduction in the number of adventitial microvessels associated with the helical stent suggesting a reduction in wall hypoxia. A

subsequent human clinical trial of patients with peripheral artery disease showed improved patency of the superficial femoral artery out to two years when treated with a helical stent compared to a straight stent (Zeller et al. 2016). All of this is consistent with recent studies from De Nisco et al. (2019) [108] suggesting the atheroprotective nature of helical flow in the coronary arteries.

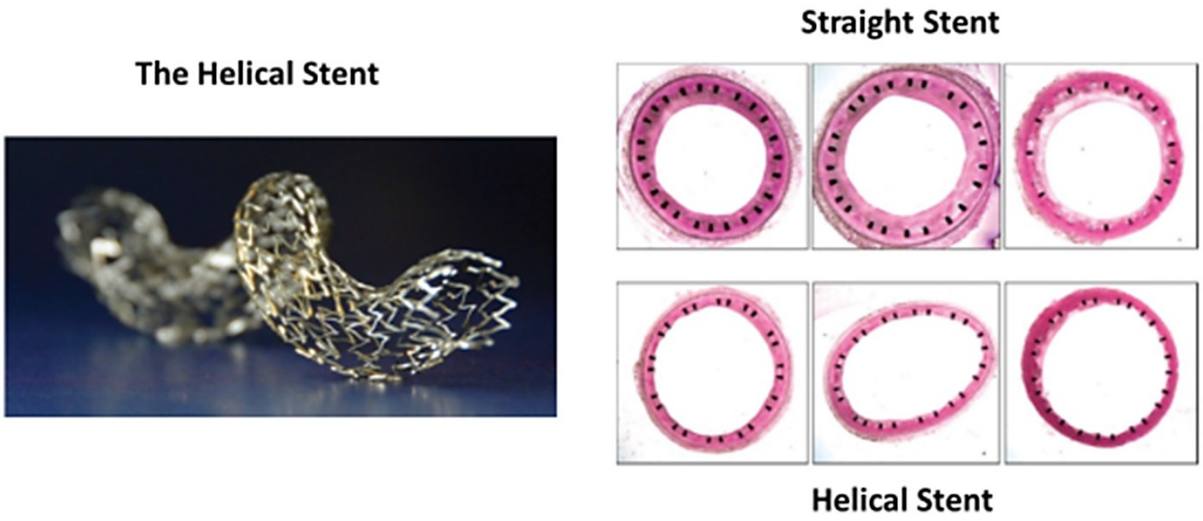

Figure 8. The helical stent reduces intimal hyperplasia. (left) Image of a helical stent [86] (right) Reduction of intimal hyperplasia 30 days after helical stent implantation in pig common carotid arteries [106].

Computer simulations of flow in the helical stent versus the straight stent [107, 109] showed that the helical stent enhances wall shear stress (WSS) and mass transfer rate (indicated by the Sherwood number Sh) significantly – about 3 fold for both WSS and Sh. Although wall oxygen tensions were not measured, it is expected that elevated mass transfer rates (Sh) reduce wall hypoxia (recall Fig. 4). Increased WSS has also been shown to suppress IH [110]([111]. It has been demonstrated that increased nitric oxide production, a normal response of endothelial cells to increased WSS, suppresses smooth muscle cell proliferation, reducing oxygen consumption, and migration from media to intima [112].These mechanisms also contribute to reduced IH in high WSS.

Summary: The Role of Oxygen Transport in Atherosclerosis and Vascular Disease

1. Hypoxia in the vascular wall leads to upregulation of the transcription factor HIF1-α that induces pro-atherogenic genes enhancing cell proliferation, inflammation, and angiogenesis.

2. Oxygen is transported to the intima and inner media from luminal blood flow and to the adventitia and outer media by vasa vasorum blood flow.

3. Elevated compressive stresses in the outer layers of the wall associated with hypertension, smoking and other cardiovascular risk factors reduce blood flow by compressing the vasa vasorum.

4. Adventitial vasa vasorum play a significant role in the initiation and progression of vascular disease.

5. dysfunctional vasa vasorum neovascularization contributes to plaque inflammation, intraplaque hemorrhage, thin-cap fibroatheromas and acute cardiovascular events.

6. Disturbed blood flow in vascular bifurcations and curvatures leads to reduced oxygen transport from blood to the inner layers of the wall. These regions of disturbed flow are associated with the development of atherosclerotic plaques.

7. HIF1-α is also activated in disturbed flow by a mechanism that is independent of hypoxia.

8. Both hypoxia and disturbed flow in regions of vessel bifurcation and curvature conspire to upregulate HIF1-α that induces vascular dysfunction and atherogenesis.

9. Vascular stenting to open a diseased blood vessel induces both outer and inner wall hypoxia which are exaggerated by stent overexpansion. This hypoxia leads to neointimal hyperplasia that may evolve to re-stenosis.

10. Inner wall hypoxia is primarily driven by the increased oxygen consumption of compressed cells (smooth muscle and fibroblasts), although disturbed flow around stent struts may reduce oxygen transport from the lumen in the early response (until the struts are covered by neo-intima). Outer wall hypoxia is secondary to vasa vasorum compression reducing blood flow to the outer layers in addition to cell compression.

11. Stent overexpansion exacerbates hypoxia by increasing wall stresses and vasa vasorum compression.

12. To overcome oxygen transport limitations from lumenal blood flow, helical stents have been developed that induce secondary flows to enhance oxygen transport rates. Early animal and human studies of the helical stent show reduced intimal hyperplasia compared to straight stents.

Acknowledgements

Disclosures

References

1. Marsch, E., J.C. Sluimer, and M.J. Daemen, *Hypoxia in atherosclerosis and inflammation.* Curr Opin Lipidol, 2013. **24**(5): p. 393-400.
2. Ferns, G.A.A. and L. Heikal, *Hypoxia in Atherogenesis.* Angiology, 2017. **68**(6): p. 472-493.
3. Semenza, G.L., *Hypoxia-inducible factors in physiology and medicine.* Cell, 2012. **148**(3): p. 399-408.
4. Bartels, K., A. Grenz, and H.K. Eltzschig, *Hypoxia and inflammation are two sides of the same coin.* Proceedings of the National Academy of Sciences, 2013. **110**(46): p. 18351.
5. Koong, A.C., E.Y. Chen, and A.J. Giaccia, *Hypoxia causes the activation of nuclear factor kappa B through the phosphorylation of I kappa B alpha on tyrosine residues.* Cancer Res, 1994. **54**(6): p. 1425-30.
6. D'Ignazio, L. and S. Rocha, *Hypoxia Induced NF-kappaB.* Cells, 2016. **5**(1).
7. Tannahill, G.M., et al., *Succinate is an inflammatory signal that induces IL-1beta through HIF-1alpha.* Nature, 2013. **496**(7444): p. 238-42.
8. D'Ignazio, L., D. Bandarra, and S. Rocha, *NF-κB and HIF crosstalk in immune responses.* The FEBS journal, 2016. **283**(3): p. 413-424.
9. Feng, S., et al., *Mechanical Activation of Hypoxia-Inducible Factor 1α Drives Endothelial Dysfunction at Atheroprone Sites.* Arteriosclerosis, Thrombosis, and Vascular Biology, 2017. **37**(11): p. 2087-2101.
10. Corcoran, S.E. and L.A.J. O'Neill, *HIF1α and metabolic reprogramming in inflammation.* The Journal of Clinical Investigation, 2016. **126**(10): p. 3699-3707.
11. Wu, D., et al., *HIF-1alpha is required for disturbed flow-induced metabolic reprogramming in human and porcine vascular endothelium.* Elife, 2017. **6**.
12. Xu, X., et al., *Snail Is a Direct Target of Hypoxia-inducible Factor 1alpha (HIF1alpha) in Hypoxia-induced Endothelial to Mesenchymal Transition of Human Coronary Endothelial Cells.* J Biol Chem, 2015. **290**(27): p. 16653-64.
13. Zhang, B., et al., *Hypoxia induces endothelial-mesenchymal transition in pulmonary vascular remodeling.* International journal of molecular medicine, 2018. **42**(1): p. 270-278.
14. Mahmoud, M.M., et al., *TWIST1 Integrates Endothelial Responses to Flow in Vascular Dysfunction and Atherosclerosis.* Circulation research, 2016. **119**(3): p. 450-462.
15. Chen, P.-Y., et al., *Endothelial-to-mesenchymal transition drives atherosclerosis progression.* The Journal of Clinical Investigation, 2015. **125**(12): p. 4514-4528.
16. Herbst, M., T.J. Holzenbein, and B. Minnich, *Characterization of the vasa vasorum in the human great saphenous vein: a scanning electron microscopy and 3D-morphometry study using vascular corrosion casts.* Microsc Microanal, 2014. **20**(4): p. 1120-33.
17. Santilli, S.M., et al., *Transarterial wall oxygen gradients at the dog carotid bifurcation.* Am J Physiol, 1995. **268**(1 Pt 2): p. H155-61.
18. Ritman, E.L. and A. Lerman, *The dynamic vasa vasorum.* Cardiovasc Res, 2007. **75**(4): p. 649-58.
19. Wolinsky, H. and S. Glagov, *Nature of species differences in the medial distribution of aortic vasa vasorum in mammals.* Circ Res, 1967. **20**(4): p. 409-21.

20. Williams, J.K., M.L. Armstrong, and D.D. Heistad, *Vasa vasorum in atherosclerotic coronary arteries: responses to vasoactive stimuli and regression of atherosclerosis.* Circ Res, 1988. **62**(3): p. 515-23.
21. Choi, B.J., et al., *Coronary endothelial dysfunction is associated with inflammation and vasa vasorum proliferation in patients with early atherosclerosis.* Arterioscler Thromb Vasc Biol, 2014. **34**(11): p. 2473-7.
22. Niinikoski, J., C. Heughan, and T.K. Hunt, *Oxygen tensions in the aortic wall of normal rabbits.* Atherosclerosis, 1973. **17**(3): p. 353-9.
23. Heistad, D.D., et al., *Regulation of blood flow to the aortic media in dogs.* J Clin Invest, 1978. **62**(1): p. 133-40.
24. Booth, R.F., et al., *Rapid development of atherosclerotic lesions in the rabbit carotid artery induced by perivascular manipulation.* Atherosclerosis, 1989. **76**(2-3): p. 257-68.
25. Martin, J.F., R.F. Booth, and S. Moncada, *Arterial wall hypoxia following thrombosis of the vasa vasorum is an initial lesion in atherosclerosis.* Eur J Clin Invest, 1991. **21**(3): p. 355-9.
26. Maurice, G., X. Wang, and J.F. Stoltz, *Linear and nonlinear elastic modelling of the deformation of vasa vasorum.* Clin Hemorheol Microcirc, 1998. **19**(4): p. 291-8.
27. Caro, C.G., et al., *Effect of cigarette smoking on the pattern of arterial blood flow: possible insight into mechanisms underlying the development of arteriosclerosis.* Lancet, 1987. **2**(8549): p. 11-3.
28. Tarnawski, M., et al., *Effect of nicotine transdermal patch on femoral artery wavespeed in healthy human subjects measured by MRI.* The Journal of Physiology 1998. **506P**: p. 16P.
29. Tarnawski, M., et al., *Noninvasive determination of local wavespeed and distensibility of the femoral artery by comb-excited Fourier velocity-encoded magnetic resonance imaging: measurements on athletic and nonathletic human subjects.* Heart Vessels, 1994. **9**(4): p. 194-201.
30. Logan, J.G., et al., *Psychological stress and arterial stiffness in Korean Americans.* J Psychosom Res, 2012. **73**(1): p. 53-8.
31. Szmigielski, C., et al., *Pulse wave velocity correlates with aortic atherosclerosis assessed with transesophageal echocardiography.* J Hum Hypertens, 2016. **30**(2): p. 90-4.
32. Fuster, V., et al., *The pathogenesis of coronary artery disease and the acute coronary syndromes (2).* N Engl J Med, 1992. **326**(5): p. 310-8.
33. Fuster, V., et al., *The pathogenesis of coronary artery disease and the acute coronary syndromes (1).* N Engl J Med, 1992. **326**(4): p. 242-50.
34. Busse, R. and I. Fleming, *Endothelial dysfunction in atherosclerosis.* J Vasc Res, 1996. **33**(3): p. 181-94.
35. Steinberg, D., *Lipoproteins and atherosclerosis. A look back and a look ahead.* Arteriosclerosis, 1983. **3**(4): p. 283-301.
36. Lin, S.J., et al., *Transendothelial transport of low density lipoprotein in association with cell mitosis in rat aorta.* Arteriosclerosis, 1989. **9**(2): p. 230-6.
37. Yin, Y., et al., *A model for the initiation and growth of extracellular lipid liposomes in arterial intima.* Am J Physiol, 1997. **272**(2 Pt 2): p. H1033-46.

38. Wilcox, J.N. and N.A. Scott, *Potential role of the adventitia in arteritis and atherosclerosis.* Int J Cardiol, 1996. **54 Suppl**: p. S21-35.
39. Barker, S.G., et al., *The influence of the adventitia on the presence of smooth muscle cells and macrophages in the arterial intima.* Eur J Vasc Endovasc Surg, 1995. **9**(2): p. 222-7.
40. Adams, C.W. and O.B. Bayliss, *The relationship between diffuse intimal thickening, medial enzyme failure and intimal lipid deposition in various human arteries.* J Atheroscler Res, 1969. **10**(3): p. 327-39.
41. Herrmann, J., et al., *Coronary vasa vasorum neovascularization precedes epicardial endothelial dysfunction in experimental hypercholesterolemia.* Cardiovasc Res, 2001. **51**(4): p. 762-6.
42. Wilson, S.H., et al., *Activated nuclear factor-kappaB is present in the coronary vasculature in experimental hypercholesterolemia.* Atherosclerosis, 2000. **148**(1): p. 23-30.
43. Nordestgaard, B.G., et al., *Different efflux pathways for high and low density lipoproteins from porcine aortic intima.* Arteriosclerosis, 1990. **10**(3): p. 477-85.
44. Tufro-McReddie, A., et al., *Oxygen regulates vascular endothelial growth factor-mediated vasculogenesis and tubulogenesis.* Dev Biol, 1997. **183**(2): p. 139-49.
45. SoRelle, R., *Two sides of the same coin: stop angiogenesis for cancer and encourage it for coronary artery disease.* Circulation, 1998. **98**(5): p. 383-4.
46. Roberts, W.G. and G.E. Palade, *Increased microvascular permeability and endothelial fenestration induced by vascular endothelial growth factor.* J Cell Sci, 1995. **108 (Pt 6)**: p. 2369-79.
47. D'Amato, R.J., et al., *Thalidomide is an inhibitor of angiogenesis.* Proc Natl Acad Sci U S A, 1994. **91**(9): p. 4082-5.
48. de Muinck, E.D. and M. Simons, *Re-evaluating therapeutic neovascularization.* J Mol Cell Cardiol, 2004. **36**(1): p. 25-32.
49. Nagy, J.A., A.M. Dvorak, and H.F. Dvorak, *VEGF-A(164/165) and PlGF: roles in angiogenesis and arteriogenesis.* Trends Cardiovasc Med, 2003. **13**(5): p. 169-75.
50. Heistad, D.D., et al., *Role of vasa vasorum in nourishment of the aortic wall.* Am J Physiol, 1981. **240**(5): p. H781-7.
51. Heistad, D.D. and M.L. Marcus, *Role of vasa vasorum in nourishment of the aorta.* Blood Vessels, 1979. **16**(5): p. 225-38.
52. Morrison, A.D., R.S. Clements, and A.I. Winegrad, *Effects of elevated glucose concentrations on the metabolism of the aortic wall.* J Clin Invest, 1972. **51**(12): p. 3114-23.
53. Kuwahara, F., et al., *Hypoxia-inducible factor-1alpha/vascular endothelial growth factor pathway for adventitial vasa vasorum formation in hypertensive rat aorta.* Hypertension, 2002. **39**(1): p. 46-50.
54. Wilson, S.H., et al., *Simvastatin preserves the structure of coronary adventitial vasa vasorum in experimental hypercholesterolemia independent of lipid lowering.* Circulation, 2002. **105**(4): p. 415-8.
55. Moulton, K.S., et al., *Angiogenesis inhibitors endostatin or TNP-470 reduce intimal neovascularization and plaque growth in apolipoprotein E-deficient mice.* Circulation, 1999. **99**(13): p. 1726-32.

56. Moulton, K.S., et al., *Inhibition of plaque neovascularization reduces macrophage accumulation and progression of advanced atherosclerosis.* Proc Natl Acad Sci U S A, 2003. **100**(8): p. 4736-41.
57. Virmani, R., et al., *Atherosclerotic plaque progression and vulnerability to rupture: angiogenesis as a source of intraplaque hemorrhage.* Arterioscler Thromb Vasc Biol, 2005. **25**(10): p. 2054-61.
58. Bates, D.O., et al., *Regulation of microvascular permeability by vascular endothelial growth factors.* J Anat, 2002. **200**(6): p. 581-97.
59. Langheinrich, A.C., et al., *Vasa vasorum and atherosclerosis - Quid novi?* Thromb Haemost, 2007. **97**(6): p. 873-9.
60. Nielsen, L.B., *Atherogenecity of lipoprotein(a) and oxidized low density lipoprotein: insight from in vivo studies of arterial wall influx, degradation and efflux.* Atherosclerosis, 1999. **143**(2): p. 229-43.
61. de Nooijer, R., et al., *Lesional overexpression of matrix metalloproteinase-9 promotes intraplaque hemorrhage in advanced lesions but not at earlier stages of atherogenesis.* Arterioscler Thromb Vasc Biol, 2006. **26**(2): p. 340-6.
62. Moreno, P.R., et al., *Plaque neovascularization is increased in ruptured atherosclerotic lesions of human aorta: implications for plaque vulnerability.* Circulation, 2004. **110**(14): p. 2032-8.
63. Yuan, X.M., et al., *Iron in human atheroma and LDL oxidation by macrophages following erythrophagocytosis.* Atherosclerosis, 1996. **124**(1): p. 61-73.
64. Lee, T.S., et al., *Erythrophagocytosis and iron deposition in atherosclerotic lesions.* Chin J Physiol, 1999. **42**(1): p. 17-23.
65. Kolodgie, F.D., et al., *Intraplaque hemorrhage and progression of coronary atheroma.* N Engl J Med, 2003. **349**(24): p. 2316-25.
66. O'Brien, K.D., et al., *Neovascular expression of E-selectin, intercellular adhesion molecule-1, and vascular cell adhesion molecule-1 in human atherosclerosis and their relation to intimal leukocyte content.* Circulation, 1996. **93**(4): p. 672-82.
67. Kolodgie, F.D., et al., *Pathologic assessment of the vulnerable human coronary plaque.* Heart, 2004. **90**(12): p. 1385-91.
68. Virmani, R., et al., *Lessons from sudden coronary death: a comprehensive morphological classification scheme for atherosclerotic lesions.* Arterioscler Thromb Vasc Biol, 2000. **20**(5): p. 1262-75.
69. Xu, J., X. Lu, and G.P. Shi, *Vasa vasorum in atherosclerosis and clinical significance.* Int J Mol Sci, 2015. **16**(5): p. 11574-608.
70. Sedding, D.G., et al., *Vasa Vasorum Angiogenesis: Key Player in the Initiation and Progression of Atherosclerosis and Potential Target for the Treatment of Cardiovascular Disease.* Front Immunol, 2018. **9**: p. 706.
71. Langheinrich, A.C., et al., *Correlation of vasa vasorum neovascularization and plaque progression in aortas of apolipoprotein E(-/-)/low-density lipoprotein(-/-) double knockout mice.* Arterioscler Thromb Vasc Biol, 2006. **26**(2): p. 347-52.
72. Ku, D.N., et al., *Pulsatile flow and atherosclerosis in the human carotid bifurcation. Positive correlation between plaque location and low oscillating shear stress.* Arteriosclerosis, 1985. **5**(3): p. 293-302.

73. Gimbrone, M.A., Jr. and G. Garcia-Cardena, *Vascular endothelium, hemodynamics, and the pathobiology of atherosclerosis.* Cardiovasc Pathol, 2013. **22**(1): p. 9-15.
74. Truskey, G., F. Yuan, and D. Katz, *Transport Phenomena in Biological Systems*. 2009, Pearson Education Ltd.
75. Zarins, C.K., et al., *Carotid bifurcation atherosclerosis. Quantitative correlation of plaque localization with flow velocity profiles and wall shear stress.* Circ Res, 1983. **53**(4): p. 502-14.
76. Tarbell, J.M., et al., *Fluid Mechanics, Arterial Disease, and Gene Expression.* Annu Rev Fluid Mech, 2014. **46**: p. 591-614.
77. Tarbell, J.M., *Mass transport in arteries and the localization of atherosclerosis.* Annu Rev Biomed Eng, 2003. **5**: p. 79-118.
78. Fournier, R., *Basic Transport Phenomena in Biomedical Engineering*. Second ed. 2007: Taylor and Francis.

.
79. Tada, S. and J.M. Tarbell, *Oxygen mass transport in a compliant carotid bifurcation model.* Ann Biomed Eng, 2006. **34**(9): p. 1389-99.
80. Moore, J.A. and C.R. Ethier, *Oxygen mass transfer calculations in large arteries.* J Biomech Eng, 1997. **119**(4): p. 469-75.
81. Qiu, Y. and J.M. Tarbell, *Numerical simulation of pulsatile flow in a compliant curved tube model of a coronary artery.* J Biomech Eng, 2000. **122**(1): p. 77-85.
82. Tsutsui, H., et al., *Intravascular ultrasound evaluation of plaque distribution at curved coronary segments.* Am J Cardiol, 1998. **81**(8): p. 977-81.
83. Fernandez Esmerats, J., et al., *Disturbed Flow Increases UBE2C (Ubiquitin E2 Ligase C) via Loss of miR-483-3p, Inducing Aortic Valve Calcification by the pVHL (von Hippel-Lindau Protein) and HIF-1alpha (Hypoxia-Inducible Factor-1alpha) Pathway in Endothelial Cells.* Arterioscler Thromb Vasc Biol, 2019. **39**(3): p. 467-481.
84. Meads, C., et al., *Coronary artery stents in the treatment of ischaemic heart disease: a rapid and systematic review.* Health Technol Assess, 2000. **4**(23): p. 1-153.
85. Caro, C.G., et al., *Intimal hyperplasia following implantation of helical-centreline and straight-centreline stents in common carotid arteries in healthy pigs: influence of intraluminal flow.* J R Soc Interface, 2013. **10**(89): p. 20130578.
86. Murphy, E.A., et al., *Oxygen Mass Transport in Stented Coronary Arteries.* Ann Biomed Eng, 2016. **44**(2): p. 508-22.
87. Cheema, A.N., et al., *Adventitial microvessel formation after coronary stenting and the effects of SU11218, a tyrosine kinase inhibitor.* J Am Coll Cardiol, 2006. **47**(5): p. 1067-75.

88. Santilli, S.M., A.S. Tretinyak, and E.S. Lee, *Transarterial wall oxygen gradients at the deployment site of an intra-arterial stent in the rabbit.* Am J Physiol Heart Circ Physiol, 2000. **279**(4): p. H1518-25.
89. Tretinyak, A.S., et al., *Supplemental oxygen reduces intimal hyperplasia after intraarterial stenting in the rabbit.* J Vasc Surg, 2002. **35**(5): p. 982-7.
90. Gomes, W.J. and E. Buffolo, *Coronary stenting and inflammation: implications for further surgical and medical treatment.* Ann Thorac Surg, 2006. **81**(5): p. 1918-25.
91. Welt, F.G. and C. Rogers, *Inflammation and restenosis in the stent era.* Arterioscler Thromb Vasc Biol, 2002. **22**(11): p. 1769-76.
92. Yeh, J.S., S.J. Oh, and C.M. Hsueh, *Frequency of Vascular Inflammation and Impact on Neointimal Proliferation of Drug Eluting Stents in Porcine Coronary Arteries.* Acta Cardiol Sin, 2016. **32**(5): p. 570-577.
93. Caputo, M., et al., *Simulation of oxygen transfer in stented arteries and correlation with in-stent restenosis.* Int J Numer Method Biomed Eng, 2013. **29**(12): p. 1373-87.
94. Van der Heiden, K., et al., *The effects of stenting on shear stress: relevance to endothelial injury and repair.* Cardiovasc Res, 2013. **99**(2): p. 269-75.
95. Li, Y., et al., *The Effect of Hyperbaric Oxygen Therapy on Myocardial Perfusion after the Implantation of Drug-Eluting Stents.* Ann Clin Lab Sci, 2018. **48**(2): p. 158-163.
96. Wan, J., et al., *Supplemental oxygen reverses hypoxia-induced smooth muscle cell proliferation by modulating HIF-alpha and VEGF levels in a rabbit arteriovenous fistula model.* Ann Vasc Surg, 2014. **28**(3): p. 725-36.
97. Sanada, J.I., et al., *An experimental study of endovascular stenting with special reference to the effects on the aortic vasa vasorum.* Cardiovasc Intervent Radiol, 1998. **21**(1): p. 45-9.
98. Vasuri, F., et al., *Nestin and WT1 expression in small-sized vasa vasorum from human normal arteries.* Histol Histopathol, 2012. **27**(9): p. 1195-202.
99. Kantor, B. and S. Mohlenkamp, *Imaging of myocardial microvasculature using fast computed tomography and three-dimensional microscopic computed tomography.* Cardiol Clin, 2003. **21**(4): p. 587-605, ix.
100. Zahedmanesh, H. and C. Lally, *Determination of the influence of stent strut thickness using the finite element method: implications for vascular injury and in-stent restenosis.* Med Biol Eng Comput, 2009. **47**(4): p. 385-93.
101. Karimi, A., M. Navidbakhsh, and R. Razaghi, *A finite element study of balloon expandable stent for plaque and arterial wall vulnerability assessment.* Journal of Applied Physics, 2014. **116**(4): p. 044701.
102. Schiavone, A., L.G. Zhao, and A.A. Abdel-Wahab, *Effects of material, coating, design and plaque composition on stent deployment inside a stenotic artery--finite element simulation.* Mater Sci Eng C Mater Biol Appl, 2014. **42**: p. 479-88.
103. Corti, A., et al., *Evaluation of Stenting-Induced Vasa Vasorum Compression: a FEM Study.* J.Royal Soc Interface (In review), 2019.
104. Im, E. and M.K. Hong, *Drug-eluting stents to prevent stent thrombosis and restenosis.* Expert Rev Cardiovasc Ther, 2016. **14**(1): p. 87-104.

105. Lee, S.Y., et al., *Prednisolone- and sirolimus-eluting stent: Anti-inflammatory approach for inhibiting in-stent restenosis.* J Biomater Appl, 2016. **31**(1): p. 36-44.
106. Shinke, T., et al., *Abstract 6059: Novel Helical Stent Design Elicits Swirling Blood Flow Pattern And Inhibits Neointima Formation In Porcine Carotid Arteries.* Circulation, 2008. **118**(suppl_18): p. S_1054-S_1054.
107. Coppola, G. and C. Caro, *Arterial geometry, flow pattern, wall shear and mass transport: potential physiological significance.* J R Soc Interface, 2009. **6**(35): p. 519-28.
108. De Nisco, G., et al., *The Atheroprotective Nature of Helical Flow in Coronary Arteries.* Ann Biomed Eng, 2019. **47**(2): p. 425-438.
109. Coppola, G. and C. Caro, *Oxygen mass transfer in a model three-dimensional artery.* J R Soc Interface, 2008. **5**(26): p. 1067-75.
110. Kohler, T.R. and A. Jawien, *Flow affects development of intimal hyperplasia after arterial injury in rats.* Arterioscler Thromb, 1992. **12**(8): p. 963-71.
111. Kohler, T.R., et al., *Increased blood flow inhibits neointimal hyperplasia in endothelialized vascular grafts.* Circ Res, 1991. **69**(6): p. 1557-65.
112. Garanich, J.S., M. Pahakis, and J.M. Tarbell, *Shear stress inhibits smooth muscle cell migration via nitric oxide-mediated downregulation of matrix metalloproteinase-2 activity.* Am J Physiol Heart Circ Physiol, 2005. **288**(5): p. H2244-52.